Structure, Vol. 10, 1533–1540, November, 2002, ©2002 Elsevier Science Ltd. All rights reserved. PII S0969-2126(02)00884-5

# Crystal Structure of the Human Supernatant Protein Factor

**Achim Stocker,[1,3] Takashi Tomizaki,[2] Clemens Schulze-Briese,[2] and Ulrich Baumann[1]**

[1]Department of Chemistry and Biochemistry
University of Berne
Freiestrasse 3, 3012 Bern
Switzerland

[2]Paul-Scherrer-Institut
CH-5232 Villigen PSI
Switzerland

## Summary

**Supernatant protein factor (SPF) promotes the epoxidation of squalene catalyzed by microsomes. Several studies suggest its in vivo role in the cholesterol biosynthetic pathway by a yet unknown mechanism. SPF belongs to a family of lipid binding proteins called CRAL_TRIO, which include yeast phosphatidylinositol transfer protein Sec14 and tocopherol transfer protein TTP. The crystal structure of human SPF at a resolution of 1.9 Å reveals a two domain topology. The N-terminal 275 residues form a Sec14-like domain, while the C-terminal 115 residues consist of an eight-stranded jelly-roll barrel similar to that found in many viral protein structures. The ligand binding cavity has a peculiar horseshoe-like shape. Contrary to the Sec14 crystal structure, the lipid-exchange loop is in a closed conformation, suggesting a mechanism for lipid exchange.**

## Introduction

Cholesterol is not uniformly distributed in eukaryotic cells [1]. The plasma membrane accommodates the major part of the intracellular cholesterol content in cells whereas major parts of sterol biosynthetic activity are concentrated in the relatively cholesterol poor endoplasmic reticulum [2]. The conversion of squalene to squalene-(2,3)-oxide by microsomal squalene monooxygenase represents a key reaction of the cholesterol biosynthesis and is therefore tightly controlled [3, 4]. The reaction requires both the microsomal and cytosolic fraction of liver, along with $O_2$ and NADPH [5]. In 1957 Bloch and colleagues identified a 47 kDa protein in rat liver cytosol that they later termed "supernatant protein factor" (SPF) due to its ability to stimulate microsomal squalene epoxidation [6].

In a first hypothesis, it was proposed that SPF facilitates the access of substrate to specific enzyme sites by interacting with the microsomal membrane [7]. Later findings by the same group excluded a conventional squalene carrier function for SPF, suggesting an involvement of the unsaturated fatty acid moiety of anionic phospholipids in the promotion of SPF-mediated squalene uptake by microsomes [8, 9].

In 1999 our group identified a 46 kDa protein by incubating cytosol of bovine liver with radioactively labeled α-tocopherol [10]. Besides the well-known α-tocopherol transfer protein (α-TTP), another protein was labeled by this procedure and characterized by N-terminal sequencing. The human homolog of this protein was cloned and termed tocopherol associated protein (TAP) due to its ability to bind α-tocopherol [11]. However, attempts to isolate a 1:1 TAP-tocopherol complex failed.

Later, TAP was found by Arai and coworkers to be identical to SPF [12] and termed "squalene transfer protein" due to enhanced sterol production in SPF-transfected cells as well as squalene transfer activity in vitro [12]. Again, no evidence for a direct interaction of squalene with TAP/SPF was found by this group, hence the in vivo ligand specificity of SPF and its physiological role still remain unclear.

Sequence analysis indicated that TAP/SPF is a member of the widespread Sec14-like protein family having a characteristic lipid binding domain called CRAL_TRIO [13]. Prominent members of the CRAL_TRIO family are Sec14 from *Saccharomyces cerevisiae*, human α-tocopherol transfer protein and *cis*-retinal binding protein. In the human genome, there are three highly conserved homologs of TAP/SPF (GenBank entries AAF19258.1, AAF19259.1, and XP_092896.1). The physiological function of none of these genes has been characterized yet.

The crystal structure of Sec14, a phosphatidylinositol-transfer protein from yeast and prominent member of the CRAL_TRIO family, has been determined some years ago [14] in complex with β-octyl-glucoside as a lipid mimic. The Sec14 gene product plays an essential role in yeast Golgi secretory function by maintaining a Golgi phosphatidylcholine composition that permits efficient transport of proteins from this organelle [15]. The presence of a Sec14-like lipid binding domain in TAP/SPF provides an identification of a putative ligand binding site in this molecule.

The object of this study was to assess the three-dimensional structure of human TAP/SPF in order to gain a deeper understanding of its hypothetical ligand-transfer function.

Here we report the X-ray crystallographic structure of human supernatant protein factor (TAP/SPF) determined at 1.90 Å resolution, showing that the three-dimensional structure consists of an N-terminal SEC14-like domain with a horse shoe-shaped ligand binding cavity and a C-terminal jelly-roll.

## Results

TAP/SPF was crystallized in spacegroup P1 with three molecules per asymmetric unit and was refined to an $R_{free}$ of 0.228 at 1.90 Å resolution. Our current TAP/SPF model (Figure 1) comprises residues 1–397. The N-terminal three-linker amino acids from the cloning construct and the seven C-terminal amino acids are not

[3]Correspondence: achim.stocker@ibc.unibe.ch

**Key words:** crystal structure, squalene, tocopherol, phosphatidylinositol transfer protein, cral_trio

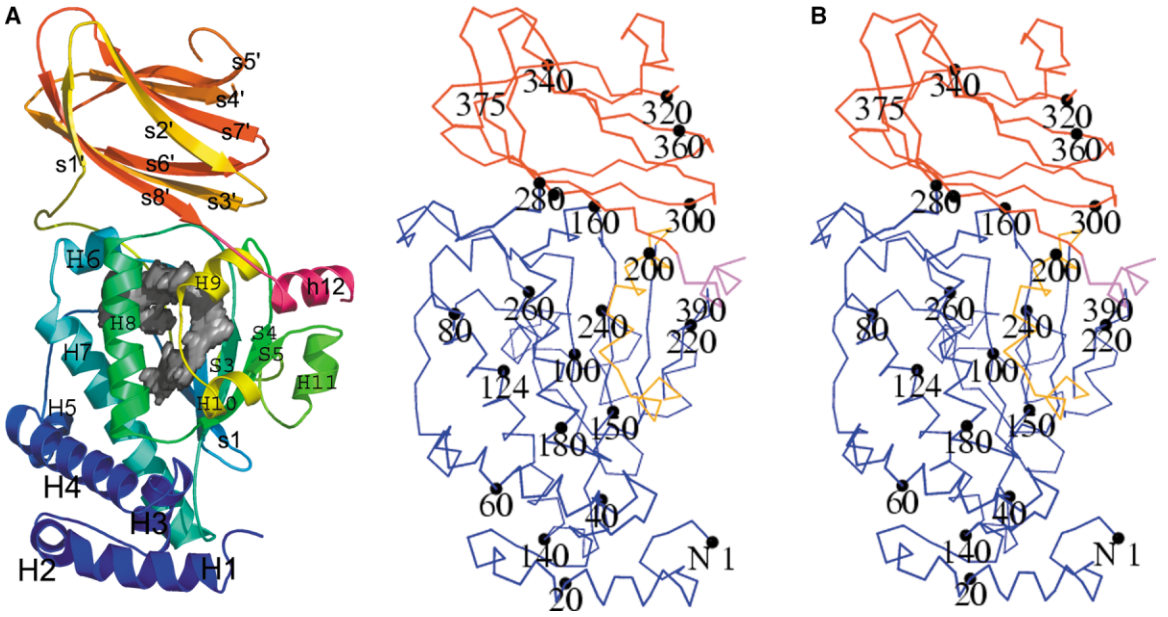


Figure 1. Crystal Structure of TAP/SPF

(A) Ribbon cartoon of TAP/SPF. The color gradient goes from blue (N terminus) to red (C terminus) with exception of the lipid-exchange loop (H9-H10) colored in yellow and the C-terminal helix shown in magenta. The Sec14 domain is in the lower part of the molecule with the lipid-exchange loop (residues 195:215) highlighted in yellow. The jelly-roll domain is on the top of the molecule. Only helices with more than three residues were included in the secondary structure. The cavity surface is shown in gray. All figures were prepared using PYMOL (Warren Delano, http://www.pymol.org).

(B) Labeled Cα trace of TAP/SPF. The SEC14 domain is shown in blue and the jelly-roll in red. The lipid exchange loop is colored yellow and the C-terminal helix magenta. The figure is rotated by 40° around the vertical compared to Figure 1A.

visible. In two of the three crystallographically independent molecules, the residues 226–232 that form a protruding loop connecting two β strands in the jelly-roll domain are disordered. The three molecules show quite substantial deviations from each other, e.g., a deviation of 0.45 Å is observed between the Cα atoms of the N-terminal domains of molecule 1 and molecule 3, and a RMS difference of 1.6 Å for the jelly-roll domains of molecules 1 and 2. Molecules 2 and 3 show RMS deviations of 0.45 and 1.7 Å for the N- and C-terminal domains, respectively. These deviations arise from rigid body movements and local distortions due to different crystal packing environments. In particular, the jelly-roll domain shows a high plasticity.

The overall structure of SPF is depicted in Figure 1 and consists of 13 β strands, 11 α helices, and 8 $3_{10}$ helices as identified by the program STRIDE [16]. Six of those $3_{10}$ helices are only three residues in length and not shown in Figure 1. SPF folds into two domains: the N-terminal 275 residues form a Sec14-like domain while the C-terminal 115 residues consist of an eight-stranded jelly-roll "barrel" similar to that found in many viral protein structures [17, 18].

## The Sec14-like Domain

The N-terminal domain consists of a central five-stranded mixed β sheet with a topology (1, 1x, 1x, 1x) where the parallel strands are connected by right-handed β-α-β motifs [19]. In this way the helices 6, 7, and 8 pack against one face of the sheet. The other side of the β sheet is mainly covered by a long loop (residues 275–300) connecting the Sec14 and jelly-roll domain. An overlay (program LSQMAN [20]) of the Sec14 structure (PDB code 1AUA) with SPF yielded a RMS deviation of 1.6 Å for 210 Cα atoms in this domain.

The central β sheet on the one side and helices 6–10 on the other side enclose a rather large (1318 Å$^3$) hydrophobic ligand binding pocket. Contrary to Sec14, however, the entrance to this cavity is blocked by helices 9 and 10 and the connecting loop. The conformation of this segment, termed hereafter lipid-exchange loop, is very different in Sec14, where the helices are rotated away from the sheet, opening the mouth of the pocket and thereby exposing an extended hydrophobic patch comprising Leu227, Phe228, and Phe231 (corresponding to Leu204, Ile205, and Phe208 in SPF) to the solvent side. This exposed hydrophobic segment is stabilized by interactions with the same residues from a symmetry-related molecule; in other words, a hydrophobic wedge consisting of the residues mentioned above is inserted into the mouth of the ligand binding pocket, hence forcing the pocket open in this crystallographic dimer of Sec14 (Figure 2).

In our TAP/SPF structure, where no such crystal contacts are observed, helix 9 is rotated by about 80° compared to Sec14, which results in a shift of about 14 Å. The hydrophobic side of helix 10 now sits on the mouth of the pocket while the more polar site faces the solvent. This conformation of segment 198–215 is further stabilized by interactions with the very C-terminal helix 13, which packs against helix 9.

The cavity itself has a peculiar horseshoe shape, dif-

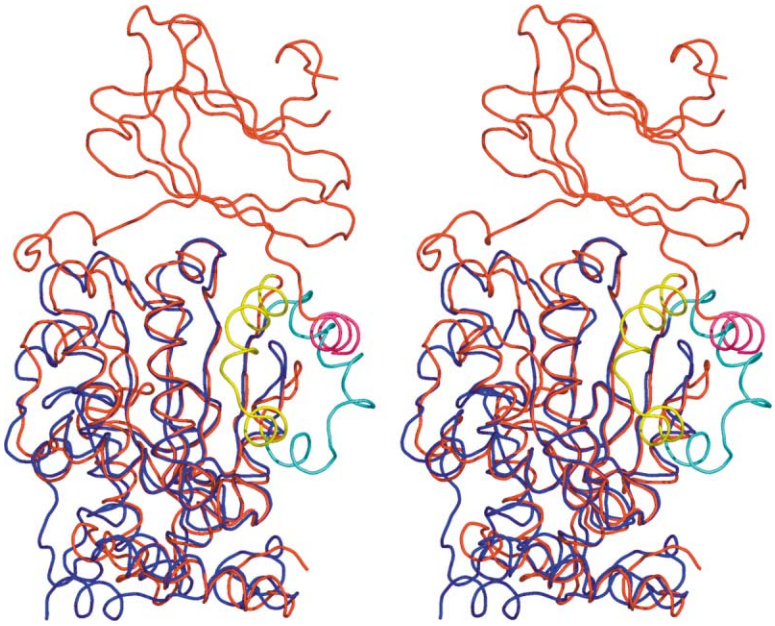

Figure 2. Overlay Sec14 (blue) and TAP/SPF (red)

The lipid-exchange loops from Sec14 (highlighted in cyan) and TAP/SPF (yellow) are in very different conformations. In TAP/SPF the loop closes the ligand binding site and is locked in this conformation by the C-terminal helix shown in magenta. The conformation observed in Sec14 in the presence of β-octylglucoside belongs probably to the membrane-associated form.

ferent from the one in Sec14. The center of the ring is occupied by two tyrosine side chains (residues 153 and 171) hydrogen bonded to each other (Figure 3), dividing in this way the pocket into two branches. The pocket is mostly lined by hydrophobic amino acid side chains. An exception is the presence of aspartic acid 101, which replaces the equivalent Glu124 in Sec14. Glu127, corresponding to Glu150 in Sec14, points now to the inside of the pocket, forming a salt bridge with Lys124, which replaces Leu147 in Sec14.

The other branch of the pocket corresponds roughly to the location where the "inner" β-octylglucoside molecule is found in the Sec14 structure. Already during the early stages of protein purification, mass spectrometry had revealed the presence of an unidentified ligand, probably originating from *E. coli*, with a mass of 349 ± 4 Da. Residual weak electron density in this part of the pocket clearly indicates the presence of an alkyl chain with length >16 carbon atoms (Figure 4), but attempts for a closer characterization of this ligand proved to be unsuccessful. For the sake of crystallographic refinement, the ligand was tentatively modeled as palmitate (mass 255.4) to fill the more continuous part of the density. The occupancy is rather low, as can be concluded from the rather high B-factors (Table 1).

## The Jelly-Roll Domain

The C-terminal residues 290–395 fold into an eight-stranded antiparallel β sandwich consisting of two four-stranded antiparallel β sheets, each with topology (–2x, −1, 2x), similar to the jelly-roll domains of many viral proteins. Performing a database search using DALI, the top hit was satellite tobacco necrosis virus (PDB code 2STV) with a Z score of 7.4 [21] and an RMS deviation of 2.7 Å for 101 $C_\alpha$ atoms. Frequently, these domains bind to specific ligands, such as cell surface-attached carbohydrate substrates for galactose oxidase and sialidase, or phospholipids on the outer side of the cell membrane for coagulation factor Va [22].

## The Ligand

Electrospray mass spectrometry was employed to examine ligand binding. The putative *E. coli* ligand of TAP/SPF was exchanged by incubating the protein in the presence of an excess of β-octylglucoside. Accordingly, a complex of phosphatidylinositol and TAP/SPF was

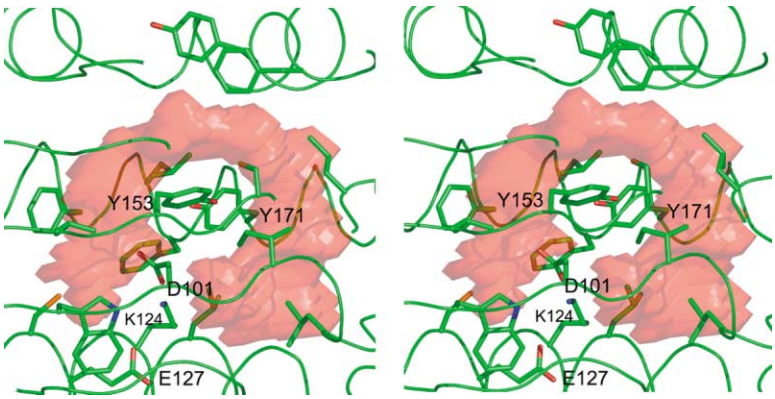


Figure 3. The Ligand Binding Cavity

The cavity surface was calculated with VOIDOO [48]. The lining is generally hydrophobic; however, some polar amino acids are present as well, e.g., Lys124, Glu127, and Asp101.

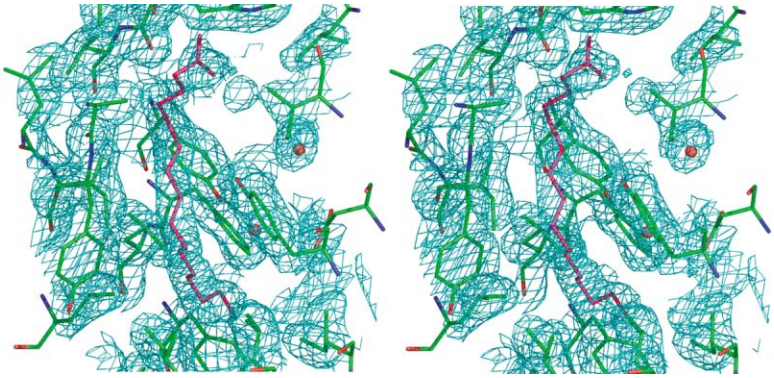

Figure 4. Stereo Figure of the Residual Electron Density of the Unknown *E. coli* Ligand

Shown is the $2F_o - F_c$ density map (cyan mesh) contoured at 1.0 sigma above the mean. The map was computed before any ligand atoms were put into the model. The ligand modeled as palmitate is shown in magenta, internal water molecules as red balls.

prepared using phospholipid liposomes. In both cases, concentrations well above the respective CMC of the compound were crucial for complex formation. Attempts to prepare ligand complexes of TAP/SPF with α-tocopherol or squalene under similar conditions proved to be unsuccessful (data not shown). The observed mass peak ratios of apo-TAP/SPF (46437 ± 4 Da) versus ligand complexes were 4:1, 4:1, and 2:1 for the *E. coli* ligand (46789 ± 4 Da), β-octylglucoside (46724.4 ± 6 Da), and phosphatidylinositol (47339.6 ± 7 Da), respectively.

Table 1. Crystallographic Statistics

| Source | SLS[d] | ID14-4[e] |
|---|---|---|
| **Data collection** | | |
| Peak wave length (Å) | 0.97884 | 0.97950 |
| No. of crystals | 2 | 1 |
| Resolution range (Å) | 20.–2.05 | 40.–1.90 |
| (Outer shell) | (2.05–2.00) | (1.95–190.) |
| No. observations | 715,326 | 660,950 |
| No. unique reflections | 184,572 | 215,407 |
| Completeness (%) | 97.1 (97.1) | 96.2 (95.2) |
| $R_{sym}$[a] | 0.093 (0.251) | 0.084 (0.257) |
| $I/\sigma$ | 15.7 (3.9) | 10.9 (4.4) |
| **Phasing** | | |
| <FOM>[c] | 0.34 | 0.31 |
| <FOM> after solvent modification | 0.58 | 0.57 |
| **Refinement** | | |
| Resolution range | 20.–2.05 | 40.–1.90 |
| No. reflections working set[b] | 177,988 | 209,964 |
| No. reflections test set | 2,836 | 4,126 |
| No. atoms total | 10,206 | 10,206 |
| Protein | 9,504 | 9,504 |
| Lipid | 52 | 52 |
| Waters | 648 | 648 |
| B-factor overall (Å$^2$) | 26.5 | 28.7 |
| Protein | 25.8 | 28.1 |
| Lipid | 50.0 | 52.2 |
| Waters | 34.1 | 36.3 |
| R (%) | 20.5 | 21.4 |
| $R_{free}$ (%) | 22.7 | 23.2 |
| RMS bonds (Å) | 0.005 | 0.005 |
| RMS angles (degrees) | 1.2 | 1.2 |

[a] $R_{sym} = \Sigma_{hkl} \Sigma_j |I(hkl;j) - \langle I(hkl) \rangle| / (\Sigma_{hkl} \Sigma_j \langle I(hkl) \rangle)$.
[b] Friedel pairs were treated as different reflections.
[c] Figure-of-merit as computed by SOLVE and RESOLVE.
[d] Swiss Light Source beam line X06SA, Villigen, Switzerland.
[e] ESRF Grenoble, beam line ID14-4.

Our data indicate that the putative *E. coli* ligand was exchanged completely by β-octylglucoside as well as by phosphatidylinositol, indicating that both compounds bind to the same site of the cavity of TAP/SPF. Nevertheless, it should be noted that this method does not allow a quantitative analysis of ligand complex formation. The peaks corresponding to the apo-protein are invariably the highest in the mass spectra, which can be interpreted either as incomplete occupancy or as dissociation of the complex due to the rather harsh conditions in the ESI-MS or during sample preparation.

## Discussion

Sec14-like proteins are crucial lipid carriers involved in the control of the lipid composition of biological membranes. These proteins regulate major steps of biosynthetic pathways of lipids by regulating the local abundance of their precursors. A subset of Sec14-like proteins are reported in Pfam (CRAL_TRIO, PF00650) and Prosite (profile, PS50191) entries. Among these proteins, the archetypical member is Sec14 from *Saccharomyces cerevisiae*. The biological function of Sec14 has been studied in detail by several groups showing that this protein maintains a reduced Golgi membrane phosphatidylcholine (PC) content, which is essential for Golgi secretory function and cell viability [15, 23, 24]. The collective data suggest that the phosphatidylcholine-bound form of Sec14 effects an essential repression of CDP-choline pathway activity in yeast Golgi membranes by inhibiting choline-phosphate cytidyltransferase (CCTase; EC 2.7.7.15).

A segment apparently crucial for lipid transfer is the lipid-exchange loop mentioned above, which consists of residues 191–215 in TAP/SPF. In Sec14, which was crystallized in the presence of β-octylglucoside, this loop adopts an open conformation exposing a hydrophobic patch to the exterior side of the molecule. This conformation in Sec14 is stabilized by dimerization of the molecules in the crystal lattice. A similar open conformation in a dimer has been observed recently in the structure of the nonhomologous *apo*-phosphatidylinositol transfer protein α (PITP-α) [25], where this conformation has been assigned to the membrane-bound form with the exposed hydrophobic residues anchoring the lipid-charged molecule to the membrane. Here, as well as described for Sec14 above, the open conforma-

tion is stabilized or possibly even induced by dimerization, where the hydrophobic lipid-exchange loop from a crystal symmetry-related molecule inserts partially into the binding pocket. On the contrary, in the crystal structure of the complex of PITP-α with phosphatidylcholine [26] ,where no such crystal interactions are observed, the lipid-exchange loop adopts a closed conformation.

The conformation of the lipid-exchange loop in our TAP/SPF structure is very different from that observed in Sec14, with the previously exposed hydrophobic patch facing the inside of the ligand binding cavity. Consequently, our TAP/SPF structure represents the "carrier"-state of the molecule, where the resident lipid molecule is enclosed in the hydrophobic pocket and the protein is not in contact with the membrane bilayer. This notion is supported by fact that TAP/SPF was isolated as a soluble monomeric molecule in the absence of detergents.

An interesting question concerns the details of the lipid exchange mechanism. A reasonable model describes the advent of the lipid-bound TAP/SPF protein at the membrane surface with the lipid-exchange loop closed. The surrounding of the lipid-exchange loop is still quite hydrophobic (solvent-exposed residues Ile296, Leu297, Phe298, and Pro299) facilitating docking to the membrane. The question arising now is whether interaction with the membrane lipids is sufficient for the opening of the lipid-exchange loop or whether dimerization is required as well. In the case of TAP/SPF, it is first necessary to push the C-terminal helix away from the lipid-exchange loop in order to open the pocket and to release the bound ligand into the membrane. In case of a lipid exchange, another lipid molecule has to get pulled out of the membrane followed by loop closure and concomitant dissociation of the complex from the membrane.

It has been reported that Sec14 localizes as a peripheral membrane protein that can be recovered in stable association with highly enriched yeast Golgi membranes [27]. In later experiments, it was shown that the N-terminal 129 residues are sufficient for Golgi targeting and colocalize with the Golgi marker KEX2p in vivo [28]. Analysis of several N-terminal Sec14-like sequences from different species revealed the presence of a segment of especially high conservation (>60%), which represents helix two of the coiled-coil motif in Sec14 (residues 56–72) as well as in TAP/SPF (residues 34–50) and α-TTP (residues 48–64). Our findings indicate that the surface segment of Sec14 that interacts with the Golgi apparatus has a common coiled-coil topology shared with TAP/SPF and several other Sec14-like proteins.

A database search showed 55% sequence similarity within 160 amino acids of the jelly-roll domain of TAP/SPF to the C-terminal extensions of squid retinal binding protein RALBP (amino acids 184–334; Swiss-Prot accession P49139), 47% similarity within 84 amino acids with the human FYVE and coiled-coil domain-containing protein (amino acids 1388–1469; GenBank AJ292348), and 39% within 141 amino acids to the human Golgi phosphoprotein GCP60 (amino acids 384–524; GenBank AB043587) and its mouse ortholog peripheral benzodiazepine receptor-associated protein (GenBank AF022770). GCP60 has previously been shown to be associated with the Golgi membrane by interaction of its C-terminal domain with the Golgi membrane protein giantin [29]. The latter could suggest that the jelly-roll domain may be involved in binding to other Golgi proteins.

TAP/SPF has been described by several groups to enhance microsomal squalene epoxidation and in consequence has led to the hypothesis that the observed stimulation includes a TAP/SPF-mediated transfer of squalene between separate membranes. The original squalene transfer hypothesis was coupled to the idea that this activity has an in vivo role in cholesterol biosynthesis. Due to the fact that no conventional protein carrier function or squalene binding could be detected, the same authors modified their hypothesis in such a way that TAP/SPF stimulates the cholesterol biosynthesis in a more indirect way by controlling the microsomal squalene uptake. It was then reported that enhanced microsomal squalene uptake mediated by TAP/SPF requires the presence of anionic phospholipids such as phosphatidylinositol, which forms a stable complex with TAP/SPF, and that the capacity of the anionic phospholipids to bind to TAP/SPF parallels their ability to enhance the stimulatory activity of TAP/SPF [30]. In agreement with these later reports, we did not find any sign of a physical interaction between TAP/SPF and squalene, but instead we could show physical binding to phosphatidylinositol. Altogether this leads us to speculate that the abundance of the cholesterol precursor squalene in the microsomal membrane seems to depend on the presence of TAP/SPF and phosphatidylinositol, which in turn may show up as key elements in the regulation of the de novo synthesis of cholesterol in eukaryotes.

It will be important to determine whether interactions involving the jelly-roll domain have a role in targeting TAP/SPF to specific cellular sites. The nature of the supposed physical partners of TAP/SPF as well as the mechanism of lipid bilayer modifications is yet to be elucidated. It should now be possible to design structure-based mutations that alter protein-ligand interactions as well as subcellular targeting in order to allow studies on the physiological significance of this protein.

## Biological Implications

Sec14-like proteins are lipid carriers of vital importance that are involved in phospholipid metabolism, signal transduction, and vesicular trafficking [31]. They form a rather large protein family called CRAL_TRIO [13], including, for example, Sec14 from yeast and human α-tocopherol transfer protein [32]. So far, from this family only the three-dimensional structure of Sec14 has been determined [14]. Here we report the crystal structure of human tocopherol-associated protein/supernatant protein factor (TAP/SPF), a protein that enhances cholesterol biosynthesis by stimulation of the squalene epoxidase activity and that binds to phospholipids.

TAP/SPF consists of two domains: the N-terminal ligand binding domain shows the typical Sec14 fold where the ligand binding site resides in a cavity between the central β sheet and the surrounding helices. Two important differences to Sec14 are notable: (i) the cavity

has a peculiar horseshoe-like shape with two tyrosine side chains in the center, and (ii) the entrance to the binding site is closed. While in Sec14 dimerization via crystal symmetry stabilizes an open conformation, we find in our structure that the segment 196–215 (called lipid-exchange loop) adopts a different conformation in such a way that the hydrophobic patch, which is exposed in the open form, now faces the ligand binding cavity. This conformation is stabilized further by the C-terminal helix of the C-terminal jelly-roll domain. The N terminus of TAP/SPF is similar to Sec14 consisting of a conserved three-helix coil, which is responsible for the localization at the Golgi apparatus. The C-terminal 120 amino acids fold into an eight-stranded jelly-roll β sandwich similar to the folding motif frequently found in viral proteins or receptor binding domains. The function of this domain is not clear now, but it is tempting to speculate that it mediates binding to a further Golgi protein. This notion is supported by the sequence homology to the human Golgi phosphoprotein GCP60 [29].

## Experimental Procedures

### Protein Expression and Purification

The N-terminal $(His)_6$-tagged TAP/SPF overexpression vector was constructed by cloning a PCR product derived from a human cDNA library into the NdeI-EcoRI sites of the pET-28b vector. The oligonucleotide primers used for PCR were 5′-CGCGGCAGCCATATGAGC GGCAGAGTCGGCGA and 5′-CCGGAATTCTCATTTCGGGGTGCCT GCCCCCA with the NdeI and EcoRI sites underlined. The N-terminal $(His)_6$-tagged TAP/SPF construct was transformed into *E. coli* BL21-Star (DE3) (Invitrogen, Carlsbad, CA). Cells were cultured overnight with agitation at 37°C in 120 ml Luria-Bertani (LB) medium containing 30 μg/ml kanamycin. The overnight culture was used to inoculate 8 liters of LB medium (30 μg/ml kanamycin). The culture was grown at 25°C to an $OD_{600}$ of 0.5 and then induced with 1 mM isopropyl-thiogalactopyranoside (IPTG) for 12 hr. Cells were harvested by centrifugation at 5000 × g for 5 min and resuspended in 250 ml of ice-cold binding buffer (20 mM imidazole, 300 mM NaCl, 20 mM Tris-HCl [pH 7.4]). The cells were disrupted in a French press at 1500 psi and the lysate was centrifuged at 39,000 × g for 40 min to remove debris. The N-terminal $(His)_6$-tagged TAP/SPF was purified from the supernatant by affinity chromatography on 10 ml of Ni-NTA SUPERFLOW (Quiagen, Basel, Switzerland) according to the user manual. Briefly, the supernatant was loaded to the column equilibrated in binding buffer and subsequently washed with 25 volumes of wash buffer (50 mM imidazole, 300 mM NaCl, 20 mM Tris-HCl [pH 7.4]). N-terminal $(His)_6$-tagged TAP/SPF was eluted with three volumes of elution buffer (200 mM imidazole, 300 mM NaCl, 20 mM Tris-HCl [pH 7.4]) and the $(His)_6$-tag was cleaved by incubating the eluate with 20 units of thrombin protease (Amersham Pharmacia Biotech Europe GmbH, Dübendorf, Switzerland) at 4°C overnight. The protein concentration was determined by the Bradford method [33]. Typical yields were 35–40 mg of pure TAP/SPF as judged by SDS-PAGE.

### Lipid Complexes and Electrospray Mass Spectrometry

All analytical-grade chemicals as well as octyl β-D-glucopyranoside, D-α-tocopherol, and L-α-phosphatidylinositol were obtained from Sigma (St. Louis, MO). Lipid vesicles were prepared by suspending the corresponding lipid in water followed by sonication for 30 min at 4°C. All vesicle containing solutions were centrifuged for 20 min at 15,000 × g before use. Vesicels containing 10 mol% squalene or 10 mol% α-tocopherol were prepared in the same way with the exception that phosphatidylinositol and isoprenoid were dissolved in chloroform in a 10:1 molar ratio prior to solvent removal by a nitrogen stream and subsequent overnight high vacuum. Purified TAP/SPF was incubated with lipid-vesicles at RT for 2 hr in order to exchange the putative *E. coli* ligand for the corresponding lipid. Incubation conditions for lipid exchange were 1 mg (21.7 nmol) TAP/SPF and 33 μmol octyl β-D-glucopyranoside or 11 μmol phosphatidylinositol, respectively. Prior to electrospray mass spectrometry (ESI-MS), samples were dialyzed overnight against water at 4°C and then diluted in solvent containing $CH_3CN/H_2O$ (1:1 v/v) and 0.5% HCOOH.

### Crystallization

Purified TAP/SPF was equilibrated in a buffer containing 2 mM EDTA, 2 mM DTT, 40 mM NaCl, 20 mM Tris-HCl (pH 7.4) and concentrated to 20 mg/ml by Centriprep-10 (Millipore AG, Volketswil, Switzerland). The protein was checked for completeness of thrombin digestion and degradation by gelfiltration and ESI-MS. The selenomethionine (SeMet)-labeled TAP/SPF was prepared by the method of methionine biosynthesis inhibition [34] and purified as the wild-type. A substitution ratio of ~100% was determined by ESI-MS (data not shown). Native crystals of TAP/SPF were obtained at 18°C by sitting-drop vapor diffusion. Drops were set up by mixing of 1 μl of TAP/SPF solution with 4 μl of reservoir solution (containing 20% [w/v] polyethylene glycol 3350, 5% [w/v] glycerol, 200 mM NaCitrate [pH 8.3]) and equilibrated against 100 μl reservoir solution at 18°C. Crystals were observed after 7–14 days and grew to an average size of 0.05 × 0.10 × 0.20 $mm^3$. Crystals of the SeMet-labeled TAP/SPF were obtained under identical conditions. The crystals belong to the space group P1 with a = 60.34 Å, b = 84.33 Å, c = 87.06 Å, α = 116.20, β = 102.52, γ = 100.07 degrees and contain three molecules per asymmetric unit. Before data collection the crystals were flash-cooled in a nitrogen stream at 110 K after raising the glycerol concentration of the crystallization solution in steps of 5% to 20% (w/v) glycerol. Data were collected at the synchrotron beam lines ID14-4 in Grenoble and SLS (PSI Villigen) at 100 K, employing a QUANTUM-4 (ADSC, San Diego) and MAR-165 CCD (MAR Xray-research, Hamburg, Germany) detector, respectively. Oscillation ranges for each image ranged between 0.5 and 1.0 degrees with typical exposure times of 1 s per image. Crystal-to-detector distances varied from 130 mm to 250 mm.

### Structure Solution and Refinement

Since initial attempts to solve the structure by molecular replacement using the Sec14 model (PDB code 1AUA) were unsuccessful, the structure was solved by means of the SAD method using SeMet labeled protein [35, 36].

A SAD dataset was collected at the beam line X06SA at the Swiss Light Source (SLS) in Villigen. This dataset was used to solve and refine the structure initially. Later, slightly higher resolution data were collected at the ID14-14 beam line at the ESRF Grenoble. Redundant datasets were collected at the peak wavelength, which was determined experimentally by fluorescence scans. Data were integrated and scaled with MOSFLM/SCALA [37, 38] or XDS [39, 40]. Data collection statistics are given in Table 1. Twenty out of 30 expected selenium positions were determined using Shake-and-Bake version 2.1 [41]. These selenium positions were refined and phases were computed using SOLVE 2.01 [42], resulting in a figure-of-merit of 0.34 at 2.25 Å resolution. Solvent modification was effected with RESOLVE 2.01 [43] and increased the figure-of-merit to 0.58 at 2.05 Å resolution using the SLS data. The resulting electron density map was easily interpretable. Further density modification was carried out using ArpWarp [44] and concomitantly a partial model including side chains was built automatically. The resulting model was completed using O [45]. Refinement was carried out with CNS [46] against the anomalous peak data. Care was taken to partition both Friedel mates either in the test or working set. Anomalous scattering factors for selenium were refined using CNS after the model had reached an $R_{free}$ of 0.28. In the final stages of refinement, NCS restrains were removed. This procedure was judged to be valid by the drop in both R and $R_{free}$ by about 1%. The final model has good stereochemistry and only 1.3% outliers in a Ramachandran plot as defined by Kleywegt and Jones [47]. Refinement statistics are given in Table 1.

### Acknowledgments

This work has been supported by the University of Berne, Switzerland, the Kontaktgruppe für Forschungsfragen of the Basel industry

and the Berner Hochschulstiftung. The help of all the staff at the Swiss Light Source in Villigen and at ESRF Grenoble is highly appreciated. Especially the help of Joanne McCarthy from ESRF Grenoble is gratefully acknowledged. We thank Adrian Schindler and Dr. Johann Schaller for ESI-MS measurements.

Received: May 31, 2002
Revised: July 18, 2002
Accepted: July 25, 2002

## References

1. Frolov, A., Woodford, J.K., Murphy, E.J., Billheimer, J.T., and Schroeder, F. (1996). Spontaneous and protein-mediated sterol transfer between intracellular membranes. J. Biol. Chem. *271*, 16075–16083.
2. Heino, S., Lusa, S., Somerharju, P., Ehnholm, C., Olkkonen, V.M., and Ikonen, E. (2000). Dissecting the role of the golgi complex and lipid rafts in biosynthetic transport of cholesterol to the cell surface. Proc. Natl. Acad. Sci. USA *97*, 8375–8380.
3. Nakamura, Y., Sakakibara, J., Izumi, T., Shibata, A., and Ono, T. (1996). Transcriptional regulation of squalene epoxidase by sterols and inhibitors in HeLa cells. J. Biol. Chem. *271*, 8053–8056.
4. Satoh, T., Hidaka, Y., and Kamei, T. (1990). Regulation of squalene epoxidase activity in rat liver. J. Lipid Res. *31*, 2095–2101.
5. Tchen, T.T., and Bloch, K. (1957). Studies on squalene epoxidase of rat liver. J. Biol. Chem. *226*, 921–930.
6. Ferguson, J.B., and Bloch, K. (1977). Purification and properties of a soluble protein activator of rat liver squalene epoxidase. J. Biol. Chem. *252*, 5381–5385.
7. Kojima, Y., Friedlander, E.J., and Bloch, K. (1981). Protein-facilitated intermembrane transfer of squalene. Demonstration by density gradient centrifugation. J. Biol. Chem. *256*, 7235–7239.
8. Chin, J., and Bloch, K. (1985). Stimulation by unsaturated fatty acid of squalene uptake in rat liver microsomes. J. Lipid Res. *26*, 819–823.
9. Chin, J., and Bloch, K. (1984). Role of supernatant protein factor and anionic phospholipid in squalene uptake and conversion by microsomes. J. Biol. Chem. *259*, 11735–11738.
10. Stocker, A., Zimmer, S., Spycher, S.E., and Azzi, A. (1999). Identification of a novel cytosolic tocopherol-binding protein: structure, specificity, and tissue distribution. IUBMB Life *48*, 49–55.
11. Zimmer, S., Stocker, A., Sarbolouki, M.N., Spycher, S.E., Sassoon, J., and Azzi, A. (2000). A novel human tocopherol-associated protein: cloning, in vitro expression, and characterization. J. Biol. Chem. *275*, 25672–25680.
12. Shibata, N., Arita, M., Misaki, Y., Dohmae, N., Takio, K., Ono, T., Inoue, K., and Arai, H. (2001). Supernatant protein factor, which stimulates the conversion of squalene to lanosterol, is a cytosolic squalene transfer protein and enhances cholesterol biosynthesis. Proc. Natl. Acad. Sci. USA *98*, 2244–2249.
13. Bateman, A., Birney, E., Durbin, R., Eddy, S.R., Finn, R.D., and Sonnhammer, E.L. (1999). Pfam 3.1: 1313 multiple alignments and profile HMMs match the majority of proteins. Nucleic Acids Res. *27*, 260–262.
14. Sha, B., Phillips, S.E., Bankaitis, V.A., and Luo, M. (1998). Crystal structure of the Saccharomyces cerevisiae phosphatidylinositol-transfer protein. Nature *391*, 506–510.
15. Xie, Z., Fang, M., and Bankaitis, V.A. (2001). Evidence for an intrinsic toxicity of phosphatidylcholine to Sec14p-dependent protein transport from the yeast Golgi complex. Mol. Biol. Cell *12*, 1117–1129.
16. Frishman, D., and Argos, P. (1995). Knowledge-based protein secondary structure assignment. Proteins *23*, 566–579.
17. Chandrasekar, V., and Johnson, J.E. (1998). The structure of tobacco ringspot virus: a link in the evolution of icosahedral capsids in the picornavirus superfamily. Structure *6*, 157–171.
18. Ban, N., and McPherson, A. (1995). The structure of satellite panicum mosaic virus at 1.9 Å resolution. Nat. Struct. Biol. *2*, 882–890.
19. Richardson, J.S. (1981). The anatomy and taxonomy of protein structure. Adv. Protein Chem. *34*, 167–339.
20. Kleywegt, G.J., and Jones, T.A. (1997). Detecting folding motifs and similarities in protein structures. Methods Enzymol. *277*, 525–545.
21. Jones, T.A., and Liljas, L. (1984). Structure of satellite tobacco necrosis virus after crystallographic refinement at 2.5 Å resolution. J. Mol. Biol. *177*, 735–767.
22. Wendt, K.S., Vodermaier, H.C., Jacob, U., Gieffers, C., Gmachl, M., Peters, J.M., Huber, R., and Sondermann, P. (2001). Crystal structure of the APC10/DOC1 subunit of the human anaphase-promoting complex. Nat. Struct. Biol. *8*, 784–788.
23. Simon, J.P., Morimoto, T., Bankaitis, V.A., Gottlieb, T.A., Ivanov, I.E., Adesnik, M., and Sabatini, D.D. (1998). An essential role for the phosphatidylinositol transfer protein in the scission of coatomer-coated vesicles from the trans-Golgi network. Proc. Natl. Acad. Sci. USA *95*, 11181–11186.
24. Henneberry, A.L., Lagace, T.A., Ridgway, N.D., and McMaster, C.R. (2001). Phosphatidylcholine synthesis influences the diacylglycerol homeostasis required for SEC14p-dependent Golgi function and cell growth. Mol. Biol. Cell *12*, 511–520.
25. Schouten, A., Agianian, B., Westerman, J., Kroon, J., Wirtz, K.W., and Gros, P. (2002). Structure of apo-phosphatidylinositol transfer protein alpha provides insight into membrane association. EMBO J. *21*, 2117–2121.
26. Yoder, M.D., Thomas, L.M., Tremblay, J.M., Oliver, R.L., Yarbrough, L.R., and Helmkamp, G.M., Jr. (2001). Structure of a multifunctional protein. Mammalian phosphatidylinositol transfer protein complexed with phosphatidylcholine. J. Biol. Chem. *276*, 9246–9252.
27. Cleves, A.E., McGee, T.P., Whitters, E.A., Champion, K.M., Aitken, J.R., Dowhan, W., Goebl, M., and Bankaitis, V.A. (1991). Mutations in the CDP-choline pathway for phospholipid biosynthesis bypass the requirement for an essential phospholipid transfer protein. Cell *64*, 789–800.
28. Skinner, H.B., Alb, J.G., Jr., Whitters, E.A., Helmkamp, G.M., Jr., and Bankaitis, V.A. (1993). Phospholipid transfer activity is relevant to but not sufficient for the essential function of the yeast SEC14 gene product. EMBO J. *12*, 4775–4784.
29. Sohda, M., Misumi, Y., Yamamoto, A., Yano, A., Nakamura, N., and Ikehara, Y. (2001). Identification and characterization of a novel Golgi protein, GCP60, that interacts with the integral membrane protein giantin. J. Biol. Chem. *276*, 45298–45306.
30. Caras, I.W., Friedlander, E.J., and Bloch, K. (1980). Interactions of supernatant protein factor with components of the microsomal squalene epoxidase system. Binding of supernatant protein factor to anionic phospholipids. J. Biol. Chem. *255*, 3575–3580.
31. Aravind, L., Neuwald, A.F., and Ponting, C.P. (1999). Sec14p-like domains in NF1 and Dbl-like proteins indicate lipid regulation of Ras and Rho signaling. Curr. Biol. *9*, R195–197.
32. Arita, M., Sato, Y., Miyata, A., Tanabe, T., Takahashi, E., Kayden, H.J., Arai, H., and Inoue, K. (1995). Human alpha-tocopherol transfer protein: cDNA cloning, expression and chromosomal localization. Biochem. J. *306*, 437–443.
33. Bradford, M.M. (1976). A rapid and sensitive method for the quantitation of microgram quantities of protein utilizing the principle of protein-dye binding. Anal. Biochem. *72*, 248–254.
34. Van Duyne, G.D., Standaert, R.F., Karplus, P.A., Schreiber, S.L., and Clardy, J. (1993). Atomic structures of the human immunophilin FKBP-12 complexes with FK506 and rapamycin. J. Mol. Biol. *229*, 105–124.
35. Wallace, B.A., Hendrickson, W.A., and Ravikumar, K. (1990). The use of single-wavelength anomalous scattering to solve the crystal structure of a gramicidin A/caesium chloride complex. Acta Crystallogr. B *46*, 440–446.
36. Turner, M.A., Yuan, C.S., Borchardt, R.T., Hershfield, M.S., Smith, G.D., and Howell, P.L. (1998). Structure determination of selenomethionyl S-adenosylhomocysteine hydrolase using data at a single wavelength. Nat. Struct. Biol. *5*, 369–376.
37. Evans, P.R. (1999). Some notes on choices in data collection. Acta Crystallogr. D Biol. Crystallogr. *55*, 1771–1772.
38. Leslie, A.G. (1999). Integration of macromolecular diffraction data. Acta Crystallogr. D Biol. Crystallogr. *55*, 1696–1702.
39. Kabsch, W. (1988). Automatic indexing of rotation diffraction patterns. J. Appl. Cryst. *21*, 67–71.

40. Kabsch, W. (1988). Evaluation of single crystal x-ray diffraction data from a position sensitive detector. J. Appl. Crystallogr. *21*, 916–924.
41. Hauptman, H.A. (1997). Shake-and-bake: an algorithm for automatic solution ab initio of crystal structures. Methods Enzymol. *277*, 3–13.
42. Terwilliger, T.C., and Berendzen, J. (1999). Automated MAD and MIR structure solution. Acta Crystallogr. D Biol. Crystallogr. *55*, 849–861.
43. Terwilliger, T.C. (2001). Maximum-likelihood density modification using pattern recognition of structural motifs. Acta Crystallogr. D Biol. Crystallogr. *57*, 1755–1762.
44. Perrakis, A., Morris, R., and Lamzin, V.S. (1999). Automated protein model building combined with iterative structure refinement. Nat. Struct. Biol. *6*, 458–463.
45. Jones, T.A., Zou, J.Y., Cowan, S.W., and Kjeldgaard (1991). Improved methods for building protein models in electron density maps and the location of errors in these models. Acta Crystallogr. A *47*, 110–119.
46. Brunger, A.T., Adams, P.D., Clore, G.M., DeLano, W.L., Gros, P., Grosse-Kunstleve, R.W., Jiang, J.S., Kuszewski, J., Nilges, M., Pannu, N.S., et al. (1998). Crystallography & NMR system: A new software suite for macromolecular structure determination. Acta Crystallogr. D Biol. Crystallogr. *54*, 905–921.
47. Kleywegt, G.J., and Jones, T.A. (1996). Phi/psi-chology: Ramachandran revisited. Structure *4*, 1395–1400.
48. Kleywegt, G.J., and Jones, T.A. (1994). Detection, delineation, measurement and display of cavities in macromolecular structures. Acta Crystallogr. D Biol. Crystallogr. *50*, 178–185.

**Accession Numbers**

The structure has been deposited at the Protein Data Bank under ID code 106U.